2014

An Analysis of Climate Feedback Contributions to the Land/Sea Warming Contrast

Oriene S. Albert

FLORIDA STATE UNIVERSITY

COLLEGE OF ARTS AND SCIENCES

AN ANALYSIS OF CLIMATE FEEDBACK CONTRIBUTIONS TO THE LAND/SEA WARMING CONTRAST

By

ORIENE S. ALBERT

A Thesis submitted to the
Department of Earth, Ocean and Atmospheric Sciences
in partial fulfillment of the
requirements for the degree of
Master of Science

Degree Awarded:
Summer Semester, 2014

Oriene S. Albert defended this thesis on April 25, 2014.
The members of the supervisory committee were:

Ming Cai
Professor Directing Thesis

Phillip Sura
Committee Member

Guosheng Liu
Committee Member

The Graduate School has verified and approved the above-named committee members, and certifies that the thesis has been approved in accordance with university requirements.

ACKNOWLEDGMENTS

I would like to acknowledge and thank my committee members, Dr. Phillip Sura and Dr. Guosheng Liu, for all their instruction and guidance over the past few years inside the classroom and out of it. Next, I would like to thank my office companion, Sergio Sejas, for his help with any questions I had during this process. Most importantly, I would like to thank and acknowledge my major professor Dr. Ming Cai, whose knowledge, guidance, and patience has allowed me to reach this milestone in my life. He is a great mentor who is always ready and willing to help.

TABLE OF CONTENTS

LIST OF FIGURES

ABSTRACT

The land/sea warming contrast being greater than unity is a well-known phenomenon in response to anthropogenic radiative forcing. The land/sea surface warming asymmetry is essentially a result of the differing surface and boundary layer properties over the land and ocean as well as the differing cloud feedbacks. In this study, we analyze the surface temperature response over the land and ocean, using the NCAR CCSM4, to a transient 1% yr^{-1} CO_2 increase at the time of the doubling. The contributions of the external forcing (CO_2) alone and various feedbacks are diagnosed using the Climate Feedback Response Analysis Method (CFRAM). This study found that the external forcing warms the land and ocean surfaces approximately the same, which suggests that the feedbacks are responsible for the warming contrast. Furthermore, this analysis confirms that the principal contributor to the above-unity land-to-sea warming ratio is the evaporation feedback; however, the results also indicate that the sensible heat flux feedback, which favors a greater warming for the ocean, has the largest land/sea warming difference. Consequently, the findings uniquely highlight the importance of other feedbacks in establishing the above-unity land-to-sea warming ratio. Specifically, the cloud and ocean dynamics/heat storage feedbacks are key contributors to the maintenance of the land/sea warming asymmetry. The results of this study provide a more holistic understanding of the climate feedbacks and their significance to the land and ocean temperature responses, when the climate is forced.

CHAPTER ONE

INTRODUCTION

1.1 Climate Change and Land/Sea Warming Contrast

'Climate change' refers to a change in the state of the climate that can be identified by changes in the mean and/or the variability of its properties, which persist for an extended period. Climate change may be due to internal processes and/or external forcings such as changes in solar radiation and volcanism or changes in composition of the atmosphere due to human activity. While many factors continue to influence climate, scientists have determined that human activities have become a dominant force, and are responsible for most of the warming observed over the past 50 years. Human-induced climate change is manifesting in the form of global warming due to an anthropogenic increase in the concentration of greenhouse gases, especially carbon dioxide (CO_2). The realization that Earth's climate sensitivity, defined by the global mean surface temperature change in response to a doubling of CO_2 atmospheric concentrations, to the greenhouse effect is more than a century old (Bony et al. 2006). However, gaining further understanding is of the utmost importance, as it can have profound impacts on our ecosystems as well as human civilizations.

The 'greenhouse effect' refers to an induced warming of the Earth's surface and troposphere as a result of a reduction of outgoing long-wave radiation (OLR) from an increase in the opaqueness of the atmosphere. Trenberth et al. 2007 showed that there was an increase in CO_2 concentrations that corresponded to an increase in anthropogenic emissions of CO_2, and Fig. 1.1 illustrates the fact that increased CO_2 concentrations have been associated with a corresponding increase in the global mean temperature.

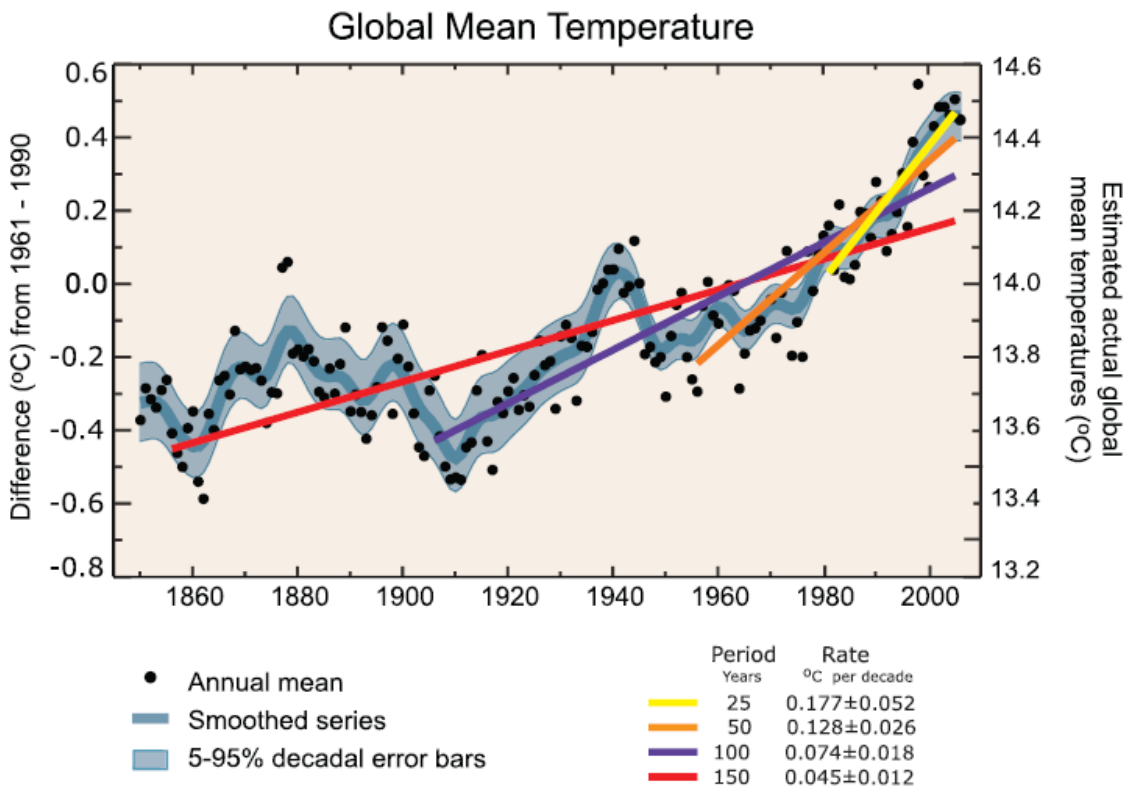

Figure 1.1 Annual global mean observed temperatures1 (black dots) along with simple fits to the data. The left hand axis shows anomalies relative to the 1961to 1990 average and the right hand axis shows the estimated actual temperature (°C). Linear trend fits to the last 25 (yellow), 50 (orange), 100 (purple) and 150 years (red) are shown, and correspond to 1981 to 2005, 1956 to 2005, 1906 to 2005, and 1856 to 2005, respectively. Note that for shorter recent periods, the slope is greater, indicating accelerated warming. The blue curve is a smoothed depiction to capture the decadal variations. To give an idea of whether the fluctuations are meaningful, decadal 5% to 95% (light grey) error ranges about that line are given. From about 1940 to 1970 the increasing industrialization increased pollution in the Northern Hemisphere, contributing to cooling, and increases in carbon dioxide and other greenhouse gases dominate the observed warming after the mid-1970s (Trenberth et al. 2007).

There is a general consensus amongst simplistic climate models as well as coupled atmosphere-ocean general circulation models, that climate simulations forced by an increase in CO_2 concentrations results in a warming of the climate (Manabe and Wetherald 1975; Ramanathan et al. 1979; Meehl et al. 2007). Furthermore, based on the Fourth Assessment Report (AR4) of the Intergovernmental Panel on Climate Change (IPCC) the climate sensitivity at equilibrium resulted in an increase in the global mean surface air temperature between 2°C

and 4.5°C (Meehl et al. 2007). An intriguing result when the climate is forced is that there is still a greater temperature response over the land surface than the ocean, regardless of whether the simulations were equilibrium or transient based, known as the 'land/sea contrast' or the 'land/sea warming ratio' (Dong et al. 2009; Manabe et al. 1991; Stouffer and Manabe 1999; Murphy and Mitchell 1995; Cubasch et al. 2001; Lambert and Chiang 2007; Meehl et al. 2007; Sutton et al. 2007; Joshi et al. 2008; Compo and Sardeshmukh 2008; Dommenget 2009).

The transient response refers to the climate response to the 1% yearly increase in CO_2 until doubled CO_2 from pre-industrial levels, before it reaches an equilibrium state (Taylor et al. 2013). Previous studies on this phenomenon revealed that the transient land/sea contrast is confined to the boundary level and occurs partially due to the different thermal inertias of the land and ocean (Manabe et al.1991; Joshi et al. 2008). The warming response of the ocean, in comparison to the land, was found to be inhibited by the fact that it can evaporate more effectively (Joshi et al. 2008; Manabe et al. 1991; Sutton et al. 2007; Joshi et al. 2013). Furthermore, the study of this warming ratio using equilibrium climate simulations has illustrated the role of the cloud amount and cloud feedbacks on the different surface and boundary layers respectively. Sutton et al. 2007 found that a reduction in the cloud amount resulted in an anomalous increase in the downward energy flux that must be balanced by an equal anomalous upward energy flux. Over the ocean this additional energy derives an increase in the evaporative cooling, while over the land the additional energy resulted in an enhancement of upward sensible and longwave heat fluxes (Sutton et al. 2007; Manabe et al. 1991). However, the enhanced evaporation cannot solely account for the observed land-favored contrast. Therefore, it is vital to gain a holistic understanding of the contributing feedbacks and processes as well as their respective roles in the maintenance of the land/sea warming ratio. This endeavor

is facilitated through the analysis of the external forcing alone as well as the effects of the climate feedbacks on the climate system.

1.2 Climate Feedbacks and Analysis Methods

The term 'feedback' in climatology typically refers to processes within the climate system that either amplify or suppress the climate system's response to an external forcing (National Research Council (NRC) 2003). A climate system is thought to be in equilibrium if it is in radiative balance but if the system is perturbed by an external forcing such as an increase in CO_2, the perturbation results in changes to processes within the system (such as changes in atmospheric and surface temperatures, atmospheric and oceanic circulations, water vapor, clouds, precipitation, evaporation, etc…) until a new equilibrium state is achieved.

In climate literature the response of the climate system to the external forcing is usually measured by the surface temperature change. Bony et al. 2006 stated that every climate variable that responds to a change in global mean surface temperature, which directly or indirectly affects the earth's radiation budget, has the potential to constitute a climate change feedback. The most commonly used methods for climate feedback analysis, such as the 'partial radiative perturbation' (PRP) method (Wetherald and Manabe 1988); 'cloud forcing analysis' (CRF) method (Cess et al. 1990, 1996); 'radiative kernel' method (Soden et al. 2008); and 'online feedback suppression' method (Hall and Manabe 1999; Schneider et al. 1999; Soden et al. 2002), are based on the premise that the temperature change is the response to radiative energy flux perturbations at the top of the atmosphere (TOA) or at the tropopause for troposphere–surface system (Ramaswamy et al. 2001; Lu and Cai 2009). Consequently, the climate feedbacks are those that directly affect the radiative budget such as water vapor, clouds, surface albedo and

atmospheric temperature etc. (Lu and Cai 2009). Another method that usually measures the strength of climate feedbacks in the same manner is the 'online feedback suppression' method (Hall and Manabe 1999; Schneider et al. 1999; Soden et al. 2002). The difference with this method is that the feedbacks do not necessarily have to be measured in the same manner, but are done so for comparison purposes and because that is the customary way to calculate climate feedbacks. For a review of these methods, excluding the radiative kernel method, readers may refer to Bony et al. (2006). One of the main shortcomings of these feedback methods is that they only provide a measure of radiative climate feedbacks, but they do not provide a measure of non-radiative feedbacks that can affect the climate sensitivity, with the exception of the online suppression feedback method. The feedback suppression approach suppresses one particular physical process in a model, which is then compared to the full model run to evaluate the feedback of that specific physical process, thus non-radiative feedbacks can also be studied. However, through the suppression of a feedback there will be "compensation effects" by other feedbacks thus resulting in incorrect evaluation of the feedbacks (Cai and Lu 2009).

The 'climate feedback-response analysis method' (CFRAM) is a relatively new method, developed by Lu and Cai (2009) and Cai and Lu (2009), that facilitates the study of climate feedbacks. This method establishes a framework in which all changes in the climate system are system responses to an external forcing, and the feedbacks are the energy flux perturbations induced by the system responses collectively (Lu and Cai 2009). Therefore climate feedbacks in this framework can be any physical process that causes an energy flux perturbation in the climate system as a response to the external forcing or subsequent feedbacks, thus including both non-radiative feedbacks and radiative feedbacks in the estimation (Lu and Cai 2009). The CFRAM allows us to calculate the partial temperature changes of each feedback in response to the energy

flux perturbations, which are additive and their total can be compared to the actual temperature change, hence their respective strengths can be measured in this framework. Furthermore, while it is known that the climate system is coupled and that the climate feedbacks are not independent from one another, the CFRAM is able to "isolate" the contributions to the total temperature change from the external forcing and each individual feedback, separately (Lu and Cai 2009, Cai and Lu 2009, and Lu and Cai 2010).

Another distinctive feature of the CFRAM is that it allows us to quantify spatial variations of climate feedbacks in a three-dimensional (3-D) structure. This feature is available because the temperature change is calculated using infrared radiation, which is explicitly and directly related to temperatures in the entire atmospheric-surface column (Lu and Cai 2009). Such a feature is essential to improving our understanding of the climate feedbacks and their contributions to the global mean climate sensitivity (Lu and Cai 2009).

In summary the CFRAM has several distinguishing features, namely, it creates a new framework where any changes in the energy cycle of the climate system (radiative and non-radiative) can be considered as climate feedbacks; it allows us to separately estimate the partial temperature changes of the external forcing and subsequent feedbacks, without relying on any information on the actual temperature change; and lastly CFRAM can be validated by summing all the partial temperature changes and evaluating how well the total agrees with the actual temperature change given by the model. For further details on this new framework please see Lu and Cai (2009) and Cai and Lu (2009).

1.3 Objective and Outline

The aforementioned studies on the asymmetrical warming between the land and ocean mainly focused on the surface energy budget to qualitatively explain this phenomenon; however, this study focuses on the quantitative analysis of the contributions from the external forcing alone as well as the individual feedbacks, over the land and ocean through the use of the CFRAM. The goal is to quantitatively estimate the importance of the different feedbacks by estimating the surface temperature change over land and ocean due to the external forcing alone and each individual feedback, which has not been undertaken before. This study would serve to further enhance our understanding of the fundamental mechanisms of the climate system as well as improve the future projections of climate change.

CHAPTER TWO

MODEL AND METHODOLOGY

2.1 Model and Data Experiments

The data used in this study are derived from the climate simulations of the National Center for Atmospheric Research (NCAR) Community Climate System Model version 4 (CCSM4). The NCAR CCSM4 is a coupled atmosphere–ocean general circulation model (GCM). The CCSM4 has an atmospheric component, the Community Atmospheric Model version 4 (CAM4), which has a finite volume dynamic core, 1° horizontal resolution, and 26 vertical levels. The ocean model is the Parallel Ocean Program version 2 (POP2) with 1° horizontal resolution enhanced to 0.27° in the equatorial region and 60 levels vertically. The CCSM4 is also comprised of the Community Land Model version 4 (CLM4), and the Community Sea Ice Code version 4 (CICE4). Additional details on the CCSM4 are provided in Gent et al. (2011). Two model simulations are analyzed: (1) A pre-industrial control simulation and (2) a 1% yr^{-1} compound CO_2 increase simulation. The CCSM4 pre-industrial control simulation runs for 1300 years holding all forcings constant at year 1850 levels, with a CO_2 concentration of 284.7 ppm. Then the 20-yr average of the annual-mean of the climate simulations between 1920 and 1940 is defined as the control (or unperturbed) climatology in the absence of the anthropogenic forcing. The second set of climate simulations is forced with an increase of CO_2 concentration at the rate at 1% yr^{-1} until the CO_2 concentration quadruples. The annual-mean climatology of the transient climate simulations is defined as the 20-yr average centered on the time of CO_2 doubling from preindustrial levels. The transient climate response to the CO_2 forcing is then given as the difference between the transient and control climatology.

2.2 A Brief Overview of the Mathematical Formulation of CFRAM

The mathematical formulation of CFRAM is based on the conservation of total energy (Lu and Cai 2009a). The energy balance equation can be represented by (in units of Wm^{-2}):

$$\mathbf{R} = \mathbf{S} + \mathbf{Q}_{\mathrm{turb}} - \mathbf{D}_{\mathrm{h}} - \mathbf{Q} \tag{2.1}$$

where $\mathbf{R}$ is the net infrared radiation leaving each layer; $\mathbf{S}$ is the solar radiation absorbed by each layer; $\mathbf{Q}_{\mathrm{turb}}$ is representative of the transfer of sensible heat from the surface to the atmosphere; $\mathbf{D}_{\mathrm{h}}$ is the transport of energy out the horizontal box into its neighbor boxes in the same layer, for each layer; $\mathbf{Q}$ is the energy storage of each layer, for an equilibrium steady state this term is zero.

Once the climate response to an external forcing, such as doubling the CO_2 concentrations, has reached an equilibrium state, the difference in the energy flux terms between the new and unperturbed equilibrium states is given by:

$$\Delta\mathbf{R} = \Delta\mathbf{S} + \Delta\mathbf{Q}_{\mathrm{turb}} - \Delta\mathbf{D}_{\mathrm{h}} - \Delta\mathbf{Q} \tag{2.2}$$

where 'Δ' stands for the difference between the two equilibrium states. To separate the different feedback processes, a linear decomposition of the solar and infrared radiation flux terms can be made giving:

$$\Delta\mathbf{S} = \Delta^{(\mathbf{CO_2})}\mathbf{S} + \Delta^{(\mathbf{wv})}\mathbf{S} + \Delta^{(\mathbf{alb})}\mathbf{S} \tag{2.3}$$

$$\Delta\mathbf{R} = \left(\frac{\partial\mathbf{R}}{\partial\mathbf{T}}\right)\Delta\mathbf{T} + \Delta^{(\mathbf{CO_2})}\mathbf{R} + \Delta^{(\mathbf{wv})}\mathbf{R} \tag{2.4}$$

In eq. (2.3), $\Delta^{(\mathbf{CO_2})}\mathbf{S}, \Delta^{(\mathbf{wv})}\mathbf{S}, \Delta^{(\mathbf{alb})}\mathbf{S}$ are the solar radiation fluxes due to the external forcing (CO_2 increase), water vapor, and surface-albedo feedbacks. In eq. (2.4), $\Delta^{(\mathbf{CO_2})}\mathbf{R}, \Delta^{(\mathbf{wv})}\mathbf{R}$ are the changes in the infrared radiative fluxes due to the external forcing and water vapor feedback, respectively, and $\left(\frac{\partial\mathbf{R}}{\partial\mathbf{T}}\right)\Delta\mathbf{T}$ is the change in the infrared radiation flux divergence in each layer due to temperature changes throughout the entire atmosphere-surface column. This linearization

is essentially a Taylor series expansion of the radiative fluxes, which does neglect the higher order terms that represent the interactions between the feedbacks in equations (2.3) and (2.4). This does introduce some error into the CFRAM, but as will be seen this error will usually be small for a small perturbation in external forcing, and the CFRAM method allows for a quantification of this error through its validation process.

Substituting equations (2.3) and (2.4) into (2.2), and rearranging terms, we obtain

$$\left(\frac{\partial \mathbf{R}}{\partial \mathbf{T}}\right)\Delta\mathbf{T} = \Delta^{(\mathbf{CO_2})}(\mathbf{S}-\mathbf{R}) + \Delta^{(\mathbf{wv})}(\mathbf{S}-\mathbf{R}) + \Delta^{(\mathbf{alb})}\mathbf{S} + \Delta\mathbf{Q}_{\mathrm{turb}} - \Delta\mathbf{D}_{\mathrm{h}} - \Delta\mathbf{Q} \tag{2.5}$$

which states that the infrared radiative energy flux perturbation due to the coupled atmosphere-surface temperature change balances the sum of the energy flux perturbations caused by the external forcing and subsequent feedbacks in each layer of the atmosphere-surface column. For the model used in this study, the terms in eq. (2.5) depend not only on the layer (in this case atmosphere or ocean), but also vary with latitude and time of year.

The first three terms on the right-hand side (RHS) of eq. (2.5) are estimated by subtracting the $1\mathrm{xCO}_2$ value of the energy flux term from the value of the energy flux term keeping all variables fixed at the $1\mathrm{xCO}_2$, except for the variable responsible for the energy flux perturbation, which is set to its $2\mathrm{xCO}_2$ value. The calculations are done according to

$$\Delta^{(\mathbf{CO_2})}(\mathbf{S}-\mathbf{R}) = (\mathbf{S}-\mathbf{R})|_{\mathbf{2xCO_2},\mathbf{T}_{1xCO_2},\mathbf{q}_{1xCO_2},alb_{1xCO_2}} - (\mathbf{S}-\mathbf{R})|_{\mathbf{1xCO_2},\mathbf{T}_{1xCO_2},\mathbf{q}_{1xCO_2},alb_{1xCO_2}} \tag{2.6}$$

$$\Delta^{(\mathbf{wv})}(\mathbf{S}-\mathbf{R}) = (\mathbf{S}-\mathbf{R})|_{\mathbf{2xCO_2},\mathbf{T}_{1xCO_2},\mathbf{q}_{1xCO_2},alb_{1xCO_2}} - (\mathbf{S}-\mathbf{R})|_{\mathbf{1xCO_2},\mathbf{T}_{1xCO_2},\mathbf{q}_{1xCO_2},alb_{1xCO_2}} \tag{2.7}$$

$$\Delta^{(\mathbf{alb})}\mathbf{S} = \mathbf{S}|_{\mathbf{2xCO_2},\mathbf{T}_{1xCO_2},\mathbf{q}_{1xCO_2},alb_{1xCO_2}} - \mathbf{S}|_{\mathbf{1xCO_2},\mathbf{T}_{1xCO_2},\mathbf{q}_{1xCO_2},alb_{1xCO_2}} \tag{2.8}$$

where $\mathbf{q}$ is the specific humidity. The rest of the terms on the RHS of eq. (2.5) are calculated directly from the difference between the $2\mathrm{xCO}_2$, and $1\mathrm{xCO}_2$, states. It is of note to mention that

these differences must be taken at a given latitude for a given time of year, and therefore this process must be done for all latitudes and days of the year used in the model.

Now, to determine the partial temperature changes associated with each of the energy flux perturbations given on the RHS of eq. (2.5) the matrix $\left(\frac{\partial \mathbf{R}}{\partial \mathbf{T}}\right)$, also known as the Planck feedback matrix, must be computed. The Planck feedback matrix is given by:

$$\left(\frac{\partial \mathbf{R}}{\partial \mathbf{T}}\right) = \begin{pmatrix} \frac{\partial \mathbf{R_a}}{\partial \mathbf{T_a}} & \frac{\partial \mathbf{R_a}}{\partial \mathbf{T_s}} \\ \frac{\partial \mathbf{R_s}}{\partial \mathbf{T_a}} & \frac{\partial \mathbf{R_s}}{\partial \mathbf{T_s}} \end{pmatrix} \tag{2.9}$$

where the subscripts 'a' and 's' represent the atmosphere and surface, respectively. The first (second) column represents the infrared radiation flux divergence in the atmospheric and surface layers due to a change in the atmospheric (surface) temperature, which is calculated by estimating the infrared radiation flux divergence at each layer due to a 1°K increase of the atmospheric (surface) temperature from its $1\text{x}CO_2$ value, using the $1\text{x}CO_2$ values for all other variables, and then subtracting from it the infrared radiation flux divergence from the $1\text{x}CO_2$ state for each corresponding layer. From here the inverse of the Planck feedback matrix can be calculated and it follows that the temperature perturbations can be solved for according to:

$$\Delta\mathbf{T} = \left(\frac{\partial \mathbf{R}}{\partial \mathbf{T}}\right)^{-1} \left\{\Delta^{(\mathbf{CO_2})}(\mathbf{S}-\mathbf{R}) + \Delta^{(wv)}(\mathbf{S}-\mathbf{R}) + \Delta^{(alb)}\mathbf{S} + \Delta\mathbf{Q}_{\text{turb}} - \Delta\mathbf{D}_{\text{h}} - \Delta\mathbf{Q}\right\} \tag{2.10}$$

The partial temperature perturbation due to the external forcing and each feedback agent,'n', can then be evaluated by,

$$\Delta\mathbf{T}^{(\text{n})} = \left(\frac{\partial \mathbf{R}}{\partial \mathbf{T}}\right)^{-1} \Delta\mathbf{F}^{(\mathbf{n})} \tag{2.11}$$

where $\Delta\mathbf{F}^{(\mathbf{n})}$ represents one of the energy flux perturbation terms on the RHS of (2.5) and $\Delta\mathbf{T}^{(\text{n})}$ is the couples atmosphere-surface temperature response to that specific energy flux

perturbation. The external focing in this study is the doubling of the CO_2 concentration, and the partial temperature response attributed directly to the external forcing is given by,

$$\Delta\mathbf{T}^{(\text{ext})} = \left(\frac{\partial\mathbf{R}}{\partial\mathbf{T}}\right)^{-\mathbf{1}} \Delta^{(\mathbf{CO_2})}(\mathbf{S}-\mathbf{R}) \tag{2.12}$$

The radiation related thermodynamic feedbacks in this study are the water vapor and surface albedo feedbacks. The partial temperature response attributed to the water vapor feedback is given by,

$$\Delta\mathbf{T}^{(\text{wv})} = \left(\frac{\partial\mathbf{R}}{\partial\mathbf{T}}\right)^{-\mathbf{1}} \Delta^{(\mathbf{wv})}(\mathbf{S}-\mathbf{R}) \tag{2.13}$$

and that of the surface-albedo feedback by,

$$\Delta\mathbf{T}^{(\text{alb})} = \left(\frac{\partial\mathbf{R}}{\partial\mathbf{T}}\right)^{-\mathbf{1}} \Delta^{(\mathbf{alb})}\mathbf{S} \tag{2.14}$$

The partial temperature response due to the large-scale dynamical feedback, given by the horizontal heat transport change, is given by,

$$\Delta\mathbf{T}^{(\text{lg\_dyn})} = -\left(\frac{\partial\mathbf{R}}{\partial\mathbf{T}}\right)^{-\mathbf{1}} \Delta\mathbf{D}_{\text{h}} \tag{2.15}$$

and that due to the local dynamical feedback, given by the sensible heat flux change, by,

$$\Delta\mathbf{T}^{(\text{loc\_dyn})} = \left(\frac{\partial\mathbf{R}}{\partial\mathbf{T}}\right)^{-\mathbf{1}} \Delta\mathbf{Q}_{\text{turb}} \tag{2.16}$$

which are non-radiative feedbacks. Finally, there is the partial temperature response due to the heat storage feedback, which is given by,

$$\Delta\mathbf{T}^{(\text{heat\_storage})} = -\left(\frac{\partial\mathbf{R}}{\partial\mathbf{T}}\right)^{-\mathbf{1}} \Delta\mathbf{Q} \tag{2.17}$$

The sum of eq. (2.12-2.17) gives the total temperature response of the climate system to the external forcing:

$$\Delta\mathbf{T}^{(\mathbf{tot})} = \Delta\mathbf{T}^{(\mathrm{ext})} + \Delta\mathbf{T}^{(\mathrm{wv})} + \Delta\mathbf{T}^{(\mathrm{alb})} + \Delta\mathbf{T}^{(\mathrm{lg\_dyn})} + \Delta\mathbf{T}^{(\mathrm{loc\_dyn})} + \Delta\mathbf{T}^{(\mathrm{heat\_storage})} \quad (2.18)$$

This is the temperature total that will be compared to the actual temperature change at each layer, so as to verify the validity of using CFRAM. The difference between the total and actual temperature changes will give an indication of how much error was introduced by the linearization of the radiative terms.

2.3 Application of the Coupled Feedback Response Analysis Method (CFRAM)

The CFRAM technique (Lu and Cai 2009; Cai and Lu 2009), which was formulated for quantifying contributions to the 3-D global warming pattern, is applied to the transient CCSM4 climate response data. The CFRAM is based on the energy balance equation of the coupled atmosphere-surface system, similar to the partial radiative perturbation (Wetherald and Manabe 1988) and radiative kernel methods (Soden and Held 2006). However, CFRAM goes beyond traditional feedback diagnostic methods by considering the temperature response to energy perturbations, due to both radiative and non-radiative feedback processes explicitly, over the entire atmospheric-surface column rather than only focusing on radiative energy perturbations at the top of the atmosphere (TOA) (Lu and Cai 2009; Cai and Lu 2009). The TOA-based feedback analysis is limited in the sense that it can only consider radiative feedback processes with non-radiative feedback processes hidden in the "lapse-rate" feedback (Lu and Cai 2009; Cai and Lu 2009).

At a given location, the atmospheric column is divided into M layers with the convention that the first layer represents the top layer of the atmosphere (for CCSM4, M=26) and the surface (either land or ocean) is the $(\mathrm{M}+1)^{th}$ layer (Lu and Cai 2009). The CFRAM equation is derived from the atmosphere-surface column energy balance equation (Lu and Cai 2009; Cai and Lu 2009) and at a latitude-longitude location can be written as

$$\Delta\mathbf{T} = \left(\frac{\partial\mathbf{R}}{\partial\mathbf{T}}\right)^{-\mathbf{1}} \begin{Bmatrix} \Delta\mathbf{F}^{ext} + \Delta^{wv}(\mathbf{S}-\mathbf{R}) + \Delta^{c}(\mathbf{S}-\mathbf{R}) + \Delta^{alb}\mathbf{S} + \Delta\mathbf{Q}^{atm\_dyn} \\ +\Delta\mathbf{Q}^{ocn\_dyn+storage} + \Delta\mathbf{Q}^{LH} + \Delta\mathbf{Q}^{SH} - \Delta^{Err}(\mathbf{S}-\mathbf{R}) \end{Bmatrix} \quad (1a)$$

The left-hand side (LHS) represents the vertical profile of the change in temperature at each atmospheric layer and surface layer. Each term inside the curly brackets represent the vertical profile of an energy flux convergence perturbation in each of the atmospheric layers and the surface layer in units of W m^{-2}. $\Delta\mathbf{F}^{ext}$ is the vertical profile of the change in radiative energy flux convergence at each atmospheric layer and at the surface layer due to the CO_2 forcing alone; the vector **S** represents the vertical profile of the solar radiation absorbed by the m^{th} atmospheric layer for $m \le$ M and at the surface layer (m=M+1); **R** is the vertical profile of the net infrared radiation flux divergence at the m^{th} atmospheric and surface layer; $\Delta^{wv}(\mathbf{S}-\mathbf{R})$ and $\Delta^{c}(\mathbf{S}-\mathbf{R})$ correspond to the vertical profiles of changes in radiative flux convergence due to changes in atmospheric water vapor and cloud properties, respectively; $\Delta^{alb}\mathbf{S}$ is the vertical profile of changes in solar energy absorbed by atmospheric layers and the surface layer due to changes in surface albedo; $\Delta^{Err}(\mathbf{S}-\mathbf{R})$ is the error in the offline radiative transfer calculation (to be discussed in detail later); $\Delta\mathbf{Q}^{LH}$ and $\Delta\mathbf{Q}^{SH}$ are changes in the energy convergence at the surface due to changes in latent and sensible heat fluxes. $\Delta\mathbf{Q}^{LH}=(0,\ldots,0,-\Delta LH)^{\mathrm{T}}$ and $\Delta\mathbf{Q}^{SH}=(0,\ldots,0,-\Delta SH)^{\mathrm{T}}$, where *LH* and *SH* denote surface turbulent latent and sensible heat fluxes, respectively,

following the traditional sign convention, namely that positive values mean upward energy flux leaving from the surface to the atmosphere; $\Delta\mathbf{Q}^{atmos\_dyn}$ is zero at the surface layer and non-zero in the atmosphere column, representing the vertical profile of the change in convergence of energy into the m^{th} layer due to non-radiative processes mainly associated with (i) convective/large-scale vertical transport of energy into the m^{th} layer from other layers in the same column, (ii) horizontal transport of energy into the m^{th} layer of the column from its neighbor columns at the same m^{th} layer, and (iii) changes in sensible and latent heat fluxes into the atmosphere; $\Delta\mathbf{Q}^{ocn\_dyn+storage}$ is zero everywhere except at the surface layer, where it represents the change in the non-radiative energy convergence mainly associated with changes in the oceanic heat transport plus heat storage. $(\partial\mathbf{R}/\partial\mathbf{T})$ is called the Planck feedback matrix whose j^{th} column represents the vertical profile of the change in divergence of LW radiative energy fluxes due to a 1°K warming at the j^{th} layer alone. Please refer to Lu and Cai 2009 Fig. 1 for an illustration of $(\partial\mathbf{R}/\partial\mathbf{T})$.

Eq. (1a) is for an analysis of the temperature change at every layer in the atmosphere and at the surface. For this study, we only study the surface temperature response ΔT_{M+1}, which is evaluated according to

$$\Delta\mathbf{T}_{\mathrm{M+1}} = \left[\left(\frac{\partial\mathbf{R}}{\partial\mathbf{T}}\right)^{-1}\right]_{\mathbf{M+1}} \begin{Bmatrix} \Delta\mathbf{F}^{ext} + \Delta^{wv}(\mathbf{S}-\mathbf{R}) + \Delta^{c}(\mathbf{S}-\mathbf{R}) + \Delta^{alb}\mathbf{S} + \Delta\mathbf{Q}^{atm\_dyn} \\ +\Delta\mathbf{Q}^{ocn\_dyn+storage} + \Delta\mathbf{Q}^{LH} + \Delta\mathbf{Q}^{SH} - \Delta^{Err}(\mathbf{S}-\mathbf{R}) \end{Bmatrix} \quad (1b)$$

where the right-hand side (RHS) is the same as before, except $\left[\left(\frac{\partial\mathbf{R}}{\partial\mathbf{T}}\right)^{-1}\right]_{\mathbf{M+1}}$ is a row vector corresponding to the M+1$^{\text{th}}$ or last row of $\left[\left(\frac{\partial\mathbf{R}}{\partial\mathbf{T}}\right)^{-1}\right]_{\mathbf{M+1}}$. In (1b) the last row of the inverse

Planck feedback matrix is multiplied with each of the terms on the right-hand side (RHS) of (1b) in brackets to obtain the partial surface temperature changes due to the CO_2 forcing alone and respective feedbacks,

$$\Delta \mathbf{T}^{(x)}_{(\mathbf{M+1})} = \left[\left(\frac{\partial \mathbf{R}}{\partial \mathbf{T}}\right)^{-\mathbf{1}}\right]_{\mathbf{M+1}} \Delta \mathbf{F}^{(\mathbf{x})} \qquad (2).$$

For an easy reference, partial temperature changes are denoted as $\Delta \mathbf{T}^{(\mathbf{x})}_{(\mathbf{M+1})}$ with the superscript "*x*" representing one of the nine superscripts from (1b). Solving (2) grid point by grid point enables us to obtain the partial surface temperature changes and comparing the total sum of individual partial temperature changes with the actual surface temperature change predicted by the original CCSM4 simulations verifies the accuracy of the CFRAM decomposition.

The Fu-Liou radiative transfer model (Fu and Liou 1992, 1993) is used for all radiation calculations in (1) for each longitude-latitude grid point using the 20-year monthly mean outputs from the control and transient climate simulations. In addition, clouds within the study are managed using a variation of the Monte Carlo Independent Column Approximation (MCICA) (Pincus et al. 2003) used previously by Taylor et al. (2011) to diagnose cloud feedback. MCICA is performed by subdividing each model grid box into 100 sub-columns and then generating cloud profiles for each. These sub-column cloud profiles are generated using a maximum-random overlap cloud generator (Raisanen et al. 2004) based on the monthly mean climatological cloud properties such as fractional cloud area, liquid and ice cloud mixing ratios, which are derived from the CCSM4 simulations. As shown previously in Taylor et al. 2013 (Fig. 1c,d) calculating each radiative term on the RHS of (1) (across all grids) using this model, results in a series of 3-D radiative energy flux perturbations thus validating the linearity assumption invoked by the CFRAM.

Standard CCSM4 outputs include 3-D solar heating and longwave cooling rates in the atmosphere and all radiative energy fluxes at the surface. The solar heating and longwave cooling rates in the CCSM4 outputs are provided in units of K day^{-1}. The heating/cooling rates in each atmospheric layer were converted from units of K day^{-1} to units of W m^{-2} by multiplying the heating/cooling rates by a factor equal to $(c_p \delta m)/86400$, where c_p is heat capacity of air at constant pressure and δm is the monthly climatological mean mass of the atmospheric layer under consideration. These outputs enable the direct quantification of errors in the offline calculations (as noted in (1)), which are defined as

$$\Delta^{Err}(\mathbf{S}-\mathbf{R}) = [\Delta(\mathbf{S}-\mathbf{R}) - \Delta(\mathbf{S}^{CCSM4} - \mathbf{R}^{CCSM4})] \quad (3)$$

where the superscript "CCSM4" indicates the results derived directly from CCSM4 output and the terms without the superscript are derived from the offline calculation. Note that the errors calculated from (3) are not due to the linearization of the radiative transfer model, but are from differences between the radiation models used; the use of 20-year monthly mean fields as inputs for the offline radiation calculations instead of instantaneous fields; and the conversion from the unit of K day^{-1} to W m^{-2}, which should be done before taking any time mean since δm varies with time.

The non-radiative energy fluxes included in the standard CCSM4 output are associated with atmospheric turbulent motions within the boundary layer (i.e., surface turbulent sensible (*SH*) and latent heat (*LH*) fluxes). All other non-radiative fluxes, such as those associated with convective and large-scale advective energy transport, are not standard output. Non-radiative energy flux perturbations and changes in heat storage are inferred using 3-D solar heating and

longwave cooling rates in an atmospheric layer m ($1 \leq m \leq$ M) from the standard output of the CCSM4 as

$$\Delta\mathbf{Q}_{\mathrm{m}}^{atm\_dyn+storage} = \Delta\mathbf{Q}_{\mathrm{m}}^{atm\_dyn} - \Delta\frac{\partial\mathbf{E}}{\partial\mathbf{t}_{\mathrm{m}}} = -\Delta(\mathbf{S}_{\mathrm{m}}^{CCSM4} - \mathbf{R}_{\mathrm{m}}^{CCSM4}) \approx \Delta\mathbf{Q}_{\mathrm{m}}^{\mathrm{atm\_dyn}} \quad (4).$$

In (4), the non-radiative or atmospheric dynamical energy flux perturbation is used to approximate the contributions from both the dynamical and heat storage term; since the heat storage term in the atmosphere is quite small it is assumed negligible. At the surface layer (m = M +1), we can evaluate the changes in net downward solar and LW radiation fluxes at the surface (m = M +1), and surface latent and sensible heat fluxes derived from the CCSM4 standard output, namely $\Delta(\mathbf{S}_{\mathrm{M+1}}^{CCSM4} - \mathbf{R}_{\mathrm{M+1}}^{CCSM4}) - \Delta\mathbf{LH} - \Delta\mathbf{SH}$. Over ocean, this term can be used to infer the change in net convergence of non-radiative energy fluxes by the ocean dynamics and ocean heat storage, namely,

$$\Delta\mathbf{Q}_{\mathrm{M+1}}^{ocn\_dyn+storage} = \Delta\mathbf{Q}_{\mathrm{M+1}}^{ocn\_dyn} - \Delta\frac{\partial\mathbf{E}}{\partial\mathbf{t}_{\mathrm{M+1}}} = -\Delta(\mathbf{S}_{\mathrm{M+1}}^{CCSM4} - \mathbf{R}_{\mathrm{M+1}}^{CCSM4}) + \Delta\mathbf{LH} + \Delta\mathbf{SH} \quad (5).$$

Over land, this term represents the change of the total energy flux convergence into the land surface layer and therefore its time mean in this transient response should be close to zero because of small land heat storage. Therefore, this term will be referred to simply as changes in ocean dynamics and ocean heat storage, although this term is not exactly zero over land.

Finally, the surface temperature change data, due to the external forcing alone and the individual feedbacks, are separated into land and ocean where only grid points that are 100% land or ocean are used, based upon the NCAR pre-industrial land fraction data, so that the

complication of coastal areas can be eliminated. Figure 2.1 illustrates the total surface temperature changes for the land (red contour) and ocean (blue contour), respectively, which were obtained from the summation of the partial temperature changes derived from the CFRAM. It is evident that these match up well with the model simulated land (black dotted) and ocean (blue dotted) surface temperature changes, which further validates the linearity assumption and provides confidence to the CFRAM results.

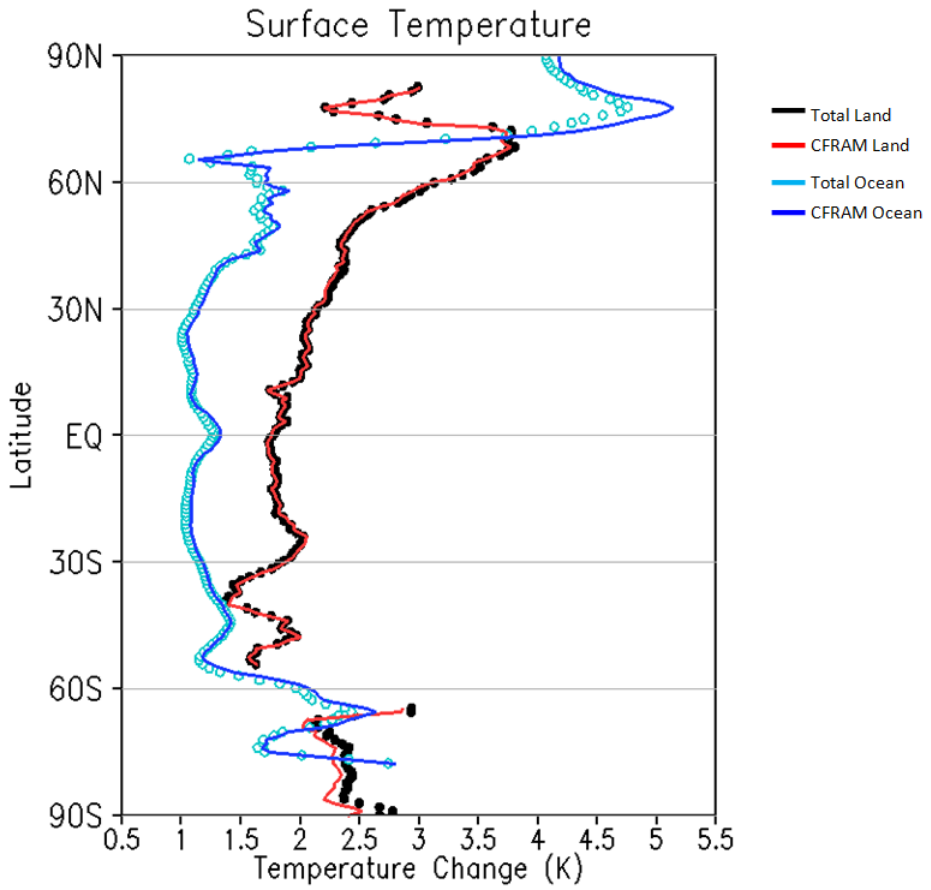

Figure 2.1 Annual-zonal mean total model temperature change and sum of CFRAM partial temperature changes.

CHAPTER THREE

RESULTS

3.1 Latitudinal and Global Mean Results

In the previous section we established confidence in the CFRAM method but in order to demonstrate the robustness of our results and analysis, the CFRAM method must first be validated. As shown in Fig. 2.1, the land and ocean model simulated time-zonal mean surface temperature changes due the doubling of CO_2, black dotted contour and light blue dotted contour respectively, match up very well with the total summed CFRAM temperature change for the land (red solid contour) and the ocean (blue solid contour), with only slight variations in the polar regions. This figure clearly illustrates the expected land/sea warming ratio with only the polar regions as an exception.

Additionally, the results produced illustrate an actual global mean temperature change of 2.304K and 1.354K for the land and ocean respectively; while the CFRAM global mean total temperature change is 2.285K and 1.398K (see Table 1). Thus, it is evident that the CFRAM is able to accurately reproduce the modeled temperature change produced in the NCAR CCSM4 climate simulation, with only marginal error that could possibly be attributed to the non-linear effect. The key feature in Fig. 2.1 is that the greatest warming occurs over the land in the tropics and mid-latitudes. In the southern hemisphere polar region the ocean warming is relatively similar to the land warming, however, the northern hemisphere polar regions experience greater polar warming over the ocean compared to the land. To ascertain how this warming ratio is achieved the temperature change contributions due to the external forcing and the feedbacks must be analyzed.

Table 1: Global Mean Temperature Changes for Individual Feedbacks over the Land and Ocean		
	Land Temperature Change (K)	**Ocean Temperature Change (K)**
Carbon Dioxide (CO_2)	1.176	1.047
Water Vapor (WV)	1.125	1.232
Ice-Albedo	0.356	0.416
Sensible Heat Flux (SH_Flux)	-1.403	0.621
Latent Heat Flux (LH_Flux)	0.182	-1.150
Ocean Dynamics+Heat Storage (Ocn_Dyn+HS)	0.009	-0.873
Clouds [SW+LW]	0.697	-0.016
Cloud Shortwave (Cloud_SW)	0.767	-0.024
Cloud Longwave (Cloud_LW)	-0.069	0.008
Offline Error	0.157	0.059
Atmospheric Dynamics (Atm_Dyn)	-0.015	0.062
Total	**2.304**	**1.354**
CFRAM Total	**2.285**	**1.398**

3.2 External Forcing and Feedback Data Results

i. External Forcing:

Let us first evaluate the resultant partial temperature change due to the external forcing, the doubling of CO_2 concentrations, alone. The surface land and ocean response to the external forcing is positive throughout, see Fig 3.1, with the land response only marginally larger than that of the ocean in the tropics, mid-latitudes and the northern hemisphere polar region. The global mean temperature change, for the land and ocean, as a result of the external forcing is noted as 1.176K and 1.047K, respectively. In the tropics the warming difference is approximately 0.05K while in the northern hemisphere mid-latitudes and the southern hemisphere polar regions, where the difference is greatest, it is approximately 0.2K. Therefore, it can be seen that the meridional warming over both land and sea is similar, which implies that the

feedback processes are likely most responsible for the meridional differences between the ocean and land warming.

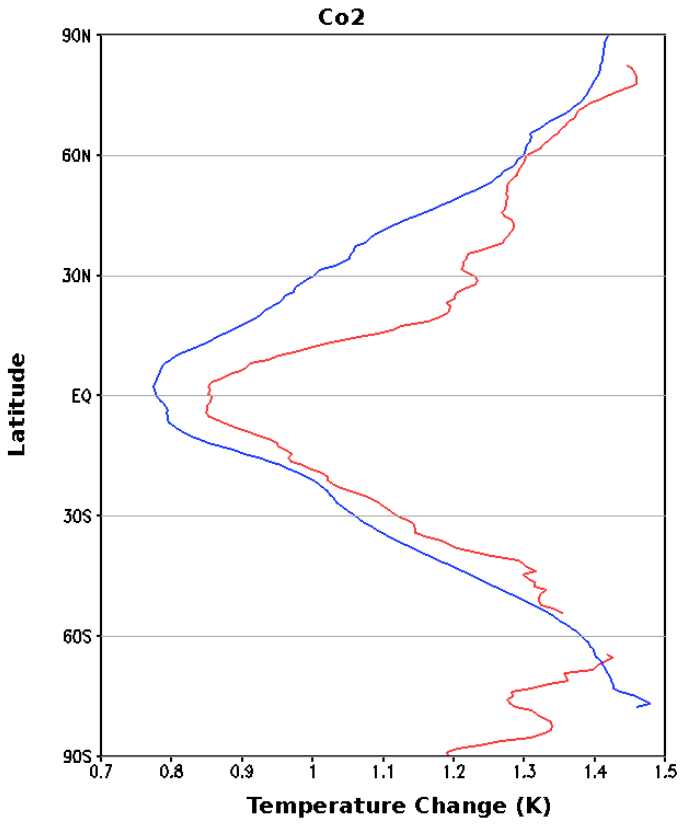

Figure 3.1 The zonal and annual-mean surface temperature response for land (red) and ocean (blue) due to the CO_2 forcing alone.

ii. Water Vapor:

Similar to the greenhouse effect of CO_2Fig 3.2 shows a positive temperature change in response to increases in atmospheric water vapor for both the land and ocean. However, unlike the external forcing, the largest increase is found in the tropics at the equator and the minimum is located in the polar region. Furthermore, the greenhouse effect due to the water vapor is much larger than that due to the doubling of CO_2 alone based on the magnitudes of the temperature change for each. Additionally, in the tropics and the sub-polar regions, the induced warming is larger for the ocean in comparison to the land. The temperature difference in the tropics is 0.6K

and ranges between 0.2K and 0.4K in the northern hemisphere mid-latitudes. The contribution of the water vapor feedback to the global mean surface temperature change is a warming of 1.125K and 1.232K for the land and ocean respectively.

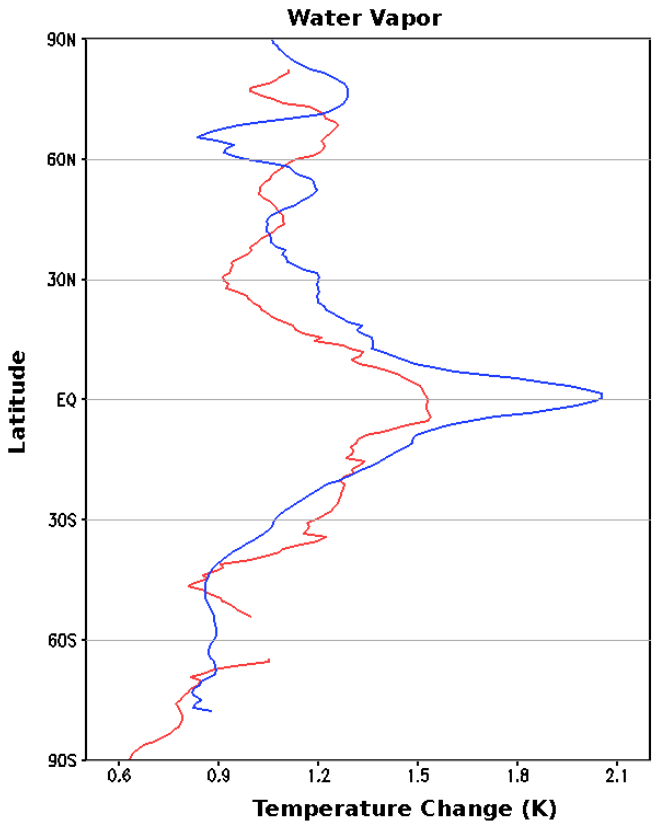

Figure 3.2 The zonal and annual-mean surface temperature response for land (red) and ocean (blue) due to the water vapor feedback.

iii. Ice-Albedo:

The contribution from the ice-albedo feedback is mainly seen in the high latitudes and the warming is shown to be dominant for the ocean, specifically in the polar regions (Fig 3.3). The largest ocean temperature warming is seen in the Arctic, with an approximate temperature increase of 5.25K, while the southern hemisphere polar region was approximately up to 3.6K. However, there is some evidence of the land warming for the northern polar region as well, although it is comparatively small. On a global scale the contribution of the ice-albedo feedback

to the mean surface temperature change for land and ocean was found to be 0.356K and 0.416K, respectively.

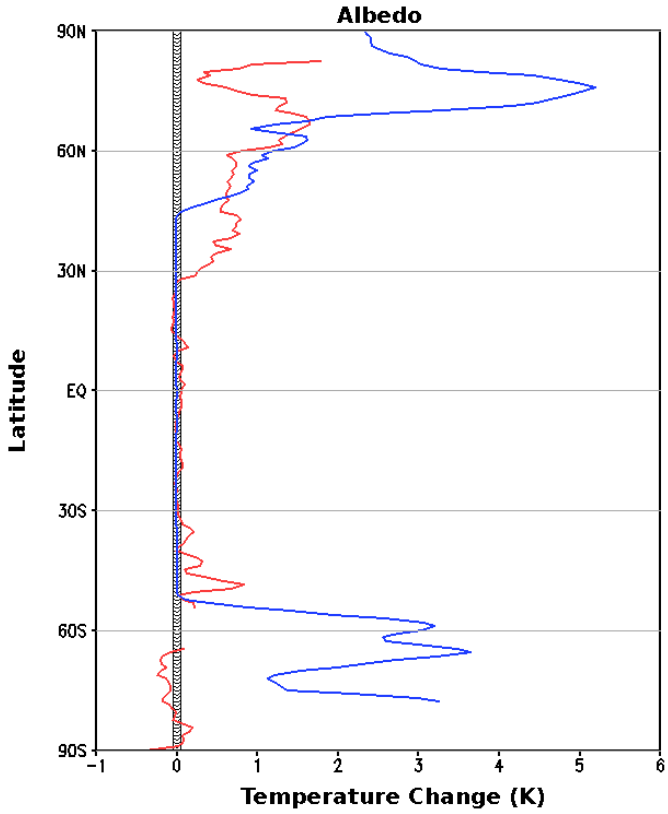

Figure 3.3 The zonal and annual-mean surface temperature response for land (red) and ocean (blue) due to the surface albedo feedback.

iv. Clouds:

Clouds provide both positive and negative contributions to the land/sea warming ratio through the longwave and shortwave components. Therefore in order to determine which contribution is dominant for this feedback we must analyze both components for both the land and ocean. Figure 3.4 illustrates a side-by-side comparison of the cloud longwave and shortwave components and we can see that for the longwave component the overall contribution is similar for both the land and ocean.

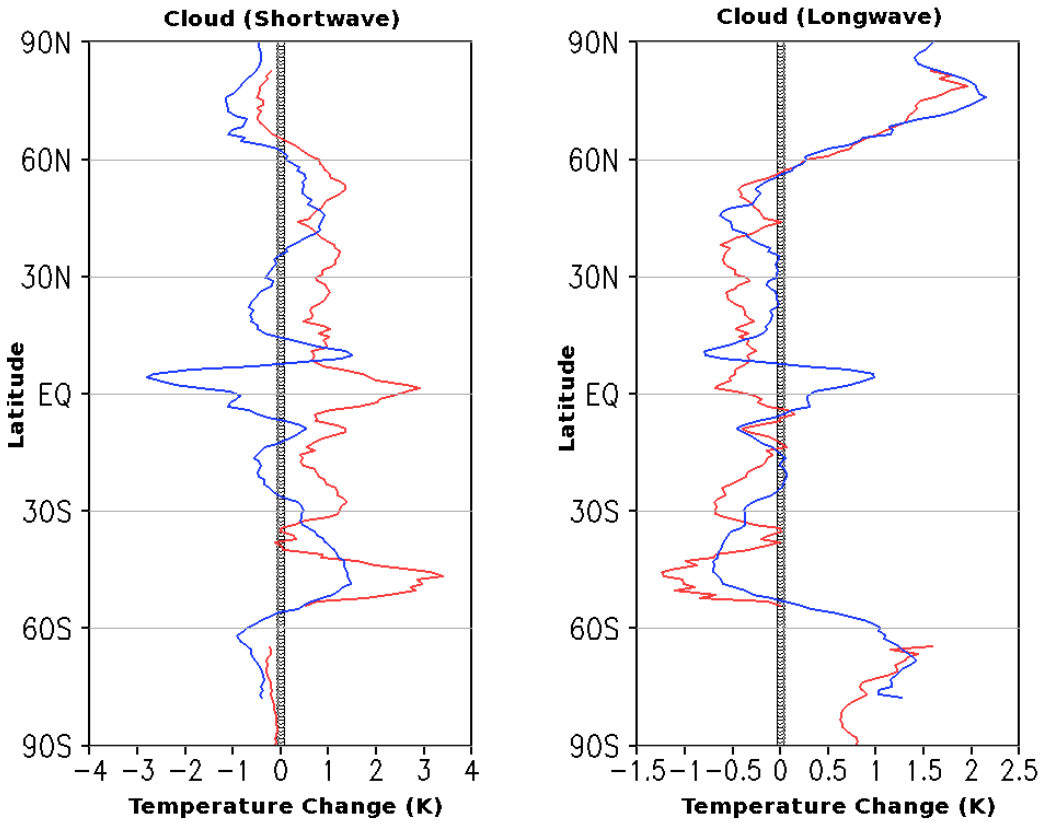

Figure 3.4 The zonal and annual-mean surface temperature response for land (red) and ocean (blue) due to the cloud shortwave and longwave feedbacks.

However, there is noteworthy warming in the polar regions, while there is cooling in the mid-latitudes and tropics except for the equatorial region of the ocean. For the shortwave component we see opposite effects for the land and the ocean in the equatorial region and also larger cooling over the ocean. When these individual components are compared to the total cloud feedback, see Fig 3.5, it is apparent that the total cloud feedback mimics the shortwave cloud component very closely, especially in the tropics and mid-latitudes, with a general cooling (warming) contribution for the ocean (land). However, the longwave effect can be seen through the warming in the poles. The global mean land temperature change for the cloud longwave and shortwave components are -0.069K and 0.767K, while for the ocean the values are 0.008K and -

0.024K, respectively. The total cloud feedback contribution for the land and ocean is 0.697K and -0.016K, respectively.

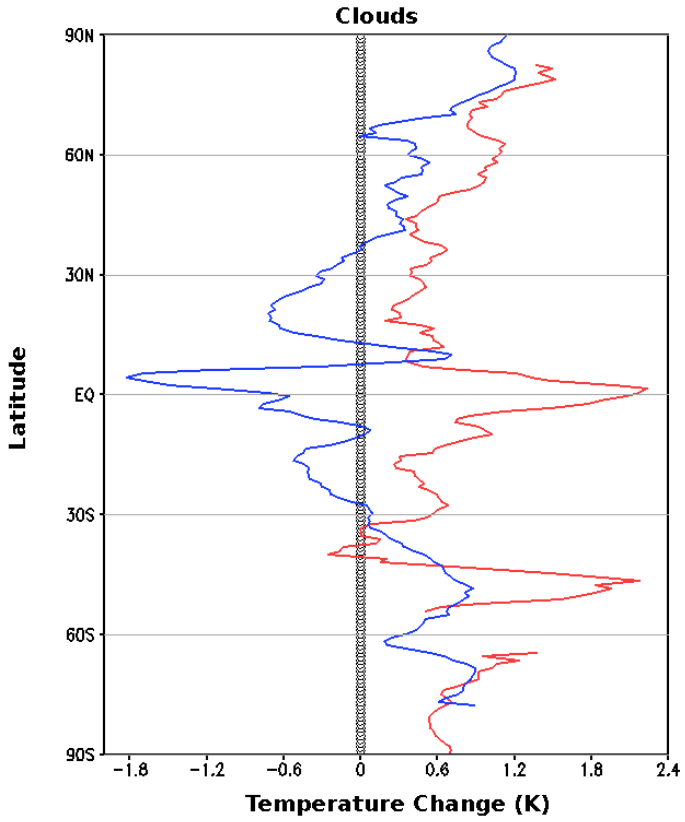

Figure 3.5 The zonal and annual-mean surface temperature response for land (red) and ocean (blue) due to the cloud feedback.

v. Sensible Heat and Latent Heat Fluxes:

Sensible heat and latent heat fluxes are similar processes which have very different effects on the land and ocean. Sensible heat flux is the process where heat energy is transferred from the Earth's surface to the atmosphere by conduction and convection while latent heat flux is the flux of heat from the Earth's surface to the atmosphere that is associated with evaporation of water at the surface. In figure 3.6 we see that there is evidence of a nominal effect in the tropics for the ocean, which greatly contrasts the land response; while there is a more noticeable temperature change response for the ocean in higher latitudes compared to the land.

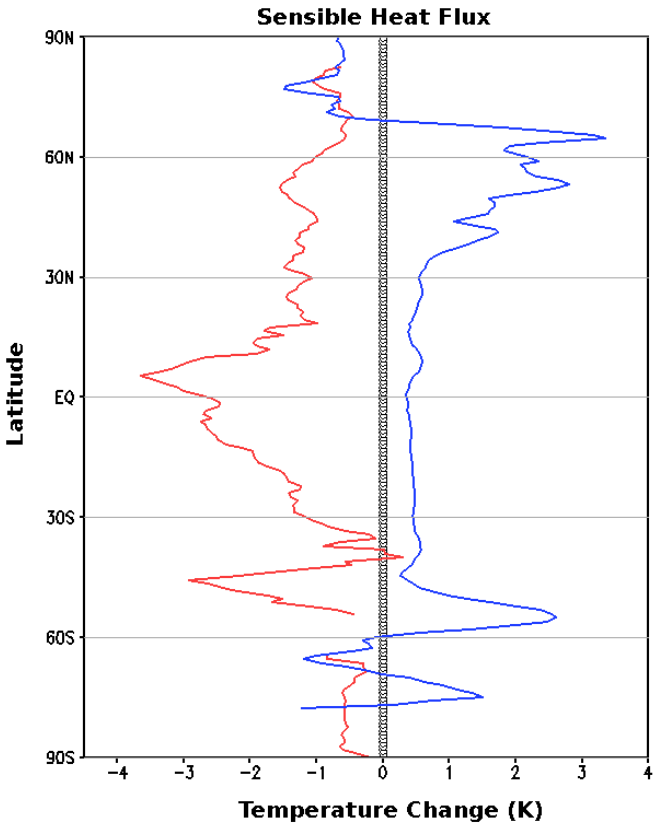

Figure 3.6 The zonal and annual-mean surface temperature response for land (red) and ocean (blue) due to the sensible heat flux feedback.

However, overall the sensible heat flux generally increases over the land but decreases over the ocean thus resulting in cooling over the land and warming over the ocean. On the other hand, the latent heat flux (Fig 3.7) illustrates an enhancement of the evaporative cooling over the ocean and a decrease over the land. This temperature change is most evident in the tropics and mid-latitudes with only slight opposition in the polar regions where some warming is shown for the ocean. On a global scale the sensible heat flux is dominant for the land with a cooling of 1.403K compared to a warming of 0.621K for the ocean; while the latent heat flux is dominant for the ocean with a temperature change of -1.150K as opposed to the land with a temperature change of 0.182K.

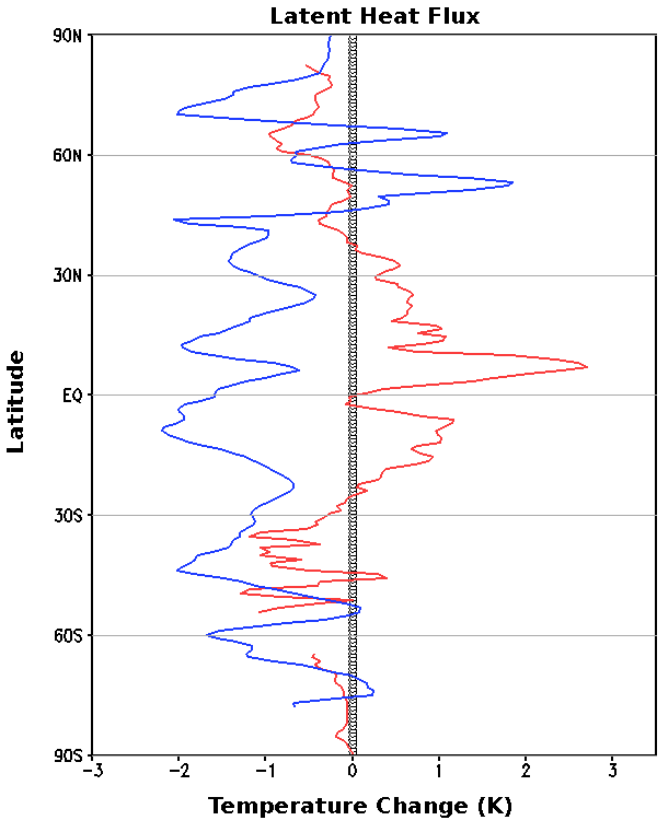

Figure 3.7 The zonal and annual-mean surface temperature response for land (red) and ocean (blue) due to the latent heat flux feedback.

vi. Atmospheric Dynamics:

The atmospheric dynamics feedback has similar effects for both the land and ocean with only minor contributions resulting in a warming of the poles and a cooling of the tropics, which would be anticipated of an enhanced poleward heat transport. However, it opposes the land/sea warming contrast as it favor a larger warming over the ocean than the land (see Fig 3.8), with the largest ocean warming occurring in the northern hemisphere polar region. Globally the mean temperature change due to the atmospheric dynamics feedback is -0.015K over the land and 0.062K over the ocean.

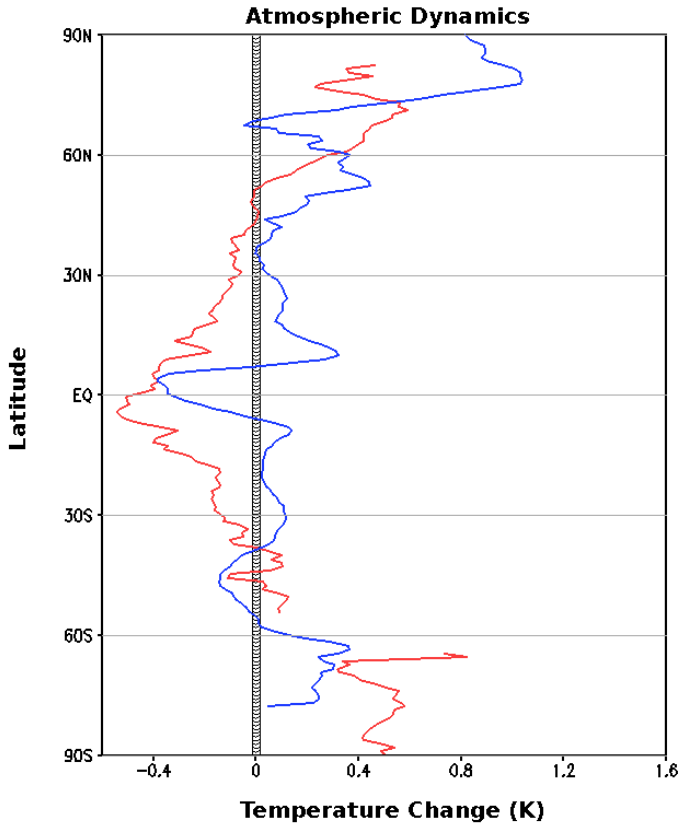

Figure 3.8 The zonal and annual-mean surface temperature response for land (red) and ocean (blue) due to the atmospheric dynamics feedback.

vii. Ocean Dynamics and Heat Storage:

As expected in figure 3.9, the land contribution of this feedback is essentially zero due to its limited heat storage capacity and has a global mean contribution of 0.009K. For the ocean this feedback illustrates a dominant cooling especially in the poles and higher latitudes with a maximum cooling of approximately 6.8K in the northern hemisphere. Although there is ocean warming in the tropics near the equator, it is negligible in comparison to the overall latitudinal contrast. The global mean temperature change for this feedback was found to be quite significant with a temperature change of -0.873K.

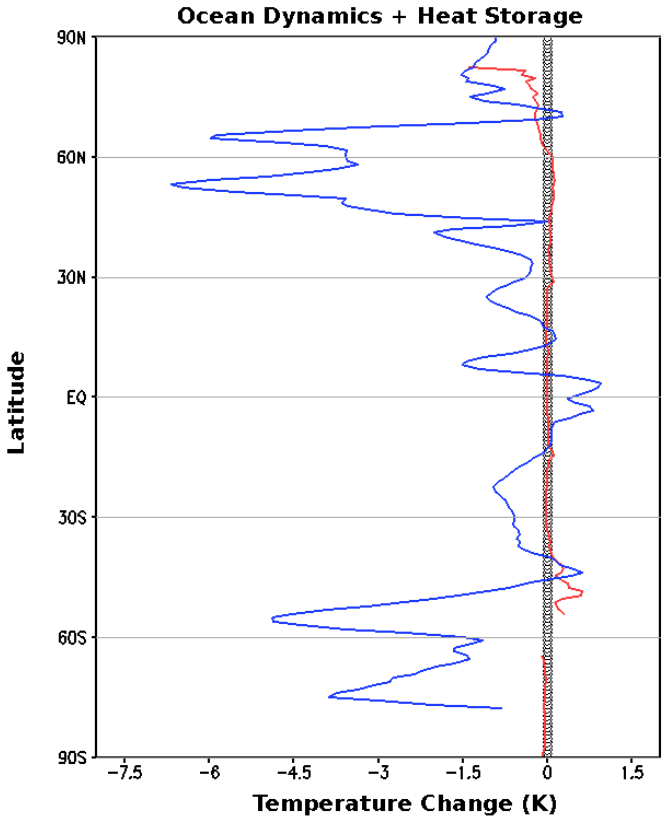

Figure 3.9 The zonal and annual-mean surface temperature response for land (red) and ocean (blue) due to the ocean dynamics/heat storage feedback.

viii. Offline Error:

Since all radiative energy flux terms were calculated in this study as an offline mode using climatological mean properties of atmospheric profiles (temperature, water vapor, and clouds) and surface albedo, differences exist between our radiative energy flux terms and the original calculations in the runtime. As a result, these differences are called offline errors. Although this study has some offline errors, the error contribution is minor with a global contribution of 0.157K and 0.059K for the land and ocean, respectively. With respect to latitudinal variation (Fig 3.10) there was evidence of cooling in the poles and warming in the tropics but the effect for the both land and the ocean are similar throughout with the exception of the polar regions, where there is evidence of a slight deviation.

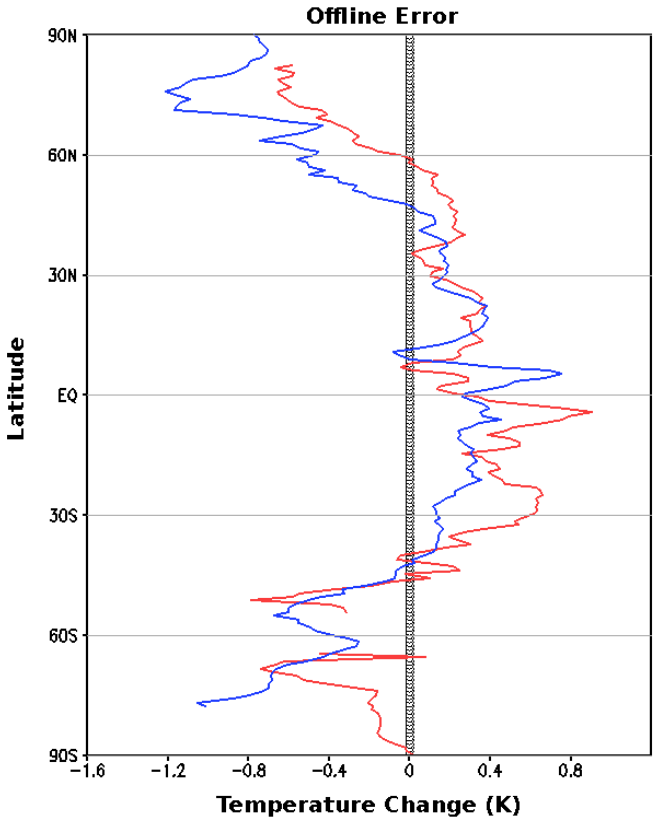

Figure 3.10 The zonal and annual-mean surface temperature response for land (red) and ocean (blue) due to the offline error in the surface temperature response.

CHAPTER FOUR

DISCUSSION

4.1 Summary of Results

The most significant feature for the total latitudinal temperature change (Fig 2.1) is the larger warming of land compared to the ocean in the tropics and mid-latitudes. Another notable feature is that the ocean warming is relatively on par with the land warming in the southern hemisphere polar region, while the Arctic experiences greater polar warming over the ocean than land. Furthermore, a latitudinal comparison of the temperature changes between land and ocean, after doubling CO_2, illustrates that the effect of the external forcing is similar for both the land and ocean but the warming response is suppressed for the ocean. The water vapor and cloud feedback contributions to the total temperature response (Fig 2.1) were dissimilar, with the water vapor feedback opposing the expected land/sea contrast. The albedo and ocean dynamics + heat storage feedbacks have substantial contributions in the polar regions for the ocean, although the temperature responses for each were contradictory to one another. Similarly, the sensible and latent heat fluxes had different effects for the land and ocean, with the sensible heat flux contributing to a considerable cooling response for the land while the latent heat flux resulted in significant cooling over the ocean. Lastly, the atmospheric dynamics feedback and the offline error contributions were found to be small in comparison with the other feedback contributions. Figure 4.1 also indicates that the key feedbacks that contribute to the land favored warming contrast are the external forcing, clouds, latent heat flux and ocean dynamics/heat storage feedbacks; while the water vapor, sensible heat flux, albedo and atmospheric dynamics feedbacks oppose it. In this discussion, emphasis will be placed on the feedbacks that greatly support or oppose total temperature change response and the land/sea warming ratio.

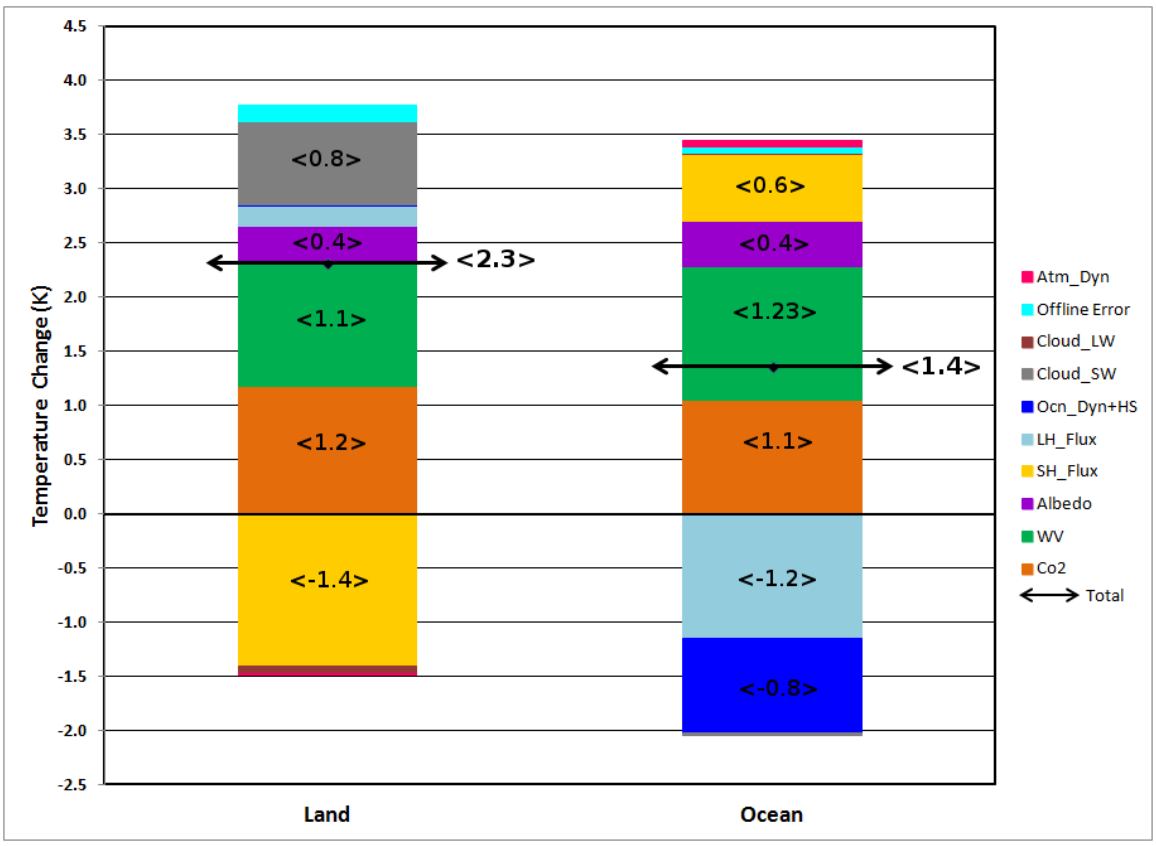

Figure 4.1 Land and ocean global mean temperature changes for each individual feedback and the actual model (Total) temperature.

4.2 Global Mean and Meridional Temperature Change Response

The multi-model study of the IPCC AR4 models by Sutton et al. (2007) provided an estimated range for the land/sea warming ratio (1.36-1.84) and the NCAR CCSM4 global annual-mean warming ratio was found to be 1.7, while the ratio based on the CFRAM is 1.64. This minor variation is likely due to the linearization used in the CFRAM calculation. To better understand how this warming ratio is achieved, the main contributors must be discerned and the CFRAM makes this analysis possible.

As stated previously, the external forcing slightly reinforces this contrast, with a 0.129K difference between the land and ocean, which is likely due to the presence of more clouds and

moisture over the ocean in the unperturbed climate mean states. Therefore, the feedbacks must have a significant influence on the warming contrast as opposed to the anthropogenic radiative forcing. The water vapor feedback, resembling the external forcing, also has a minor global temperature change variation between the land and the ocean (0.11K); however, the feedback response is favorable for a larger oceanic warming than land. The meridional profile of this feedback illustrates a descending pattern for the maximum warming at the equator and as expected from the green house effect, resulted in an overall warming for the both the land and ocean, which is representative of a larger increase in moisture and in turn an increase in the downward longwave radiation received at the surface (Taylor et al. 2013).

Another feedback that opposes the observed land/sea warming ratio is the ice-albedo feedback, which illustrates significant ocean warming in the polar regions. The pronounced polar warming in the poles is due to increased absorption of shortwave radiation at the surface as a result of the poleward retreat of snow and sea ice (Manabe et al. 1991, Sutton et al. 2007). However, the significant oceanic warming seen for this feedback, around 70°N, is not as pronounced in the total temperature response (Fig 2.1) due to the fact that it is offset by the dominant polar cooling response from the ocean dynamics/heat storage feedback. Above this latitude the warming is strong and is responsible for the larger polar warming seen over the ocean.

Similar to previous studies, the latent heat flux for the ocean surface is a significant contributor to the oceanic cooling. Studies such as Joshi et al. (2008), Manabe et al. (1991), Dong et al. (2009) and Joshi et al. (2013) attributed this cooling to the boundary layer properties of the land and ocean; the moisture limitations over land and the stomata conductance of plants. Over the land the cooling effect of the latent heat flux feedback was found to be reduced due to

the inhibited efficiency of evaporative cooling when CO_2 is doubled. When the anthropogenic forcing is increased stomata decreases and as a result transpiration and evaporation are repressed, which is noteworthy since the stomata conductance of plants is factored into the CCSM4 simulations. Additionally, the limited moisture source over land and the fact that the evaporation rate for continental surfaces is less than that over the oceans, because soil saturation is not always at 100%, constricts the evaporation feedback over land (Manabe et al. 1991; Manabe et al. 1992; Sutton et al. 2007). Lack of water vapor supplies due the constrained evaporation feedback would affect the formation of clouds and allows for more shortwave radiation to reach the surface, which likely enhances the warming response (Manabe et al. 1991). However, over the wet ocean surfaces the enhanced cooling can be attributed partially to the increased efficiency of the evaporative cooling process. The increased moisture and evaporative cooling over the oceans is likely due to an increase in saturation vapor pressure from the warming temperatures as can be expected from the Clausius-Clapeyron relationship.

Many of the aforementioned studies have concluded that the latent heat flux is one of the main contributors to the meridional land/sea warming ratio being above unity. However, this study found that the sensible heat flux feedback has the largest temperature change variation between the land and ocean, specifically in the tropics and mid-latitudes and that it greatly favors the ocean warming more than the land. Figure 3.6 illustrates a cooling contribution to the land due to an increase in the sensible heat flux, while there is a global warming of 0.62K for the ocean. In fact, when the net effect of temperature changes for these surface turbulent heat fluxes are considered, it is evident that the result is a stronger cooling effect over land of -1.22K compared to the ocean (-0.53K). Therefore, the evaporation feedback cannot be the sole

contributor to the land/sea contrast which significantly favors the land warming more than the ocean.

With respect to the global response by the cloud feedback, there is evidence of a global reduction in clouds over the land, which resulted in a warming response of 0.7K that can be attributed to the shortwave component of the total cloud feedback (Table 1). Moreover, on a global scale the longwave and shortwave effects appear to cancel each other out for the ocean, with only a -0.02K net change. Joshi et al. (2008) inferred that the significant cooling over the ocean was a result of an increase in evaporative cooling, which could imply an increase in cloud thickness. Within thick clouds the longwave and shortwave effects oppose one another and can result in an overall neutral response. Consequently, it can be said that the cloud feedback provides a significant contribution to the larger warming over land than the ocean.

This study found that the ocean dynamics/heat storage feedback is also a major contributor to the larger land warming. The ocean dynamics/heat storage feedback represents the spatial distribution of energy by oceanic circulations as well as the ocean heat storage factor. A meridional analysis of this feedback illustrated negative values in the mid-latitudes and polar regions and small positive temperature changes in the equatorial region. Positive values are mainly due to the convergence of the horizontal oceanic energy transport while negative values are due to both the divergence of the horizontal oceanic energy transport as well as an increase in the amount of heat stored, which is typically associated with downward mixing in the transient climate response (Taylor et al. 2013). The dominant cooling seen for this feedback is likely due to the combined result of an increase in the amount of heat stored and the dynamics of the Atlantic meridional circulation, which facilitates the transport of the ocean heat energy away.

Additionally, the ocean dynamics/heat storage feedback reduces the warming over the oceans globally by -0.87K, thus supporting the land/sea warming contrast being greater than 1.

Lastly, a comparison of the radiative and non-radiative feedbacks on a global scale indicated that the total effect of the external forcing, water vapor feedback, and ice-albedo feedback actually resulted in a stronger warming over oceans (2.7K) than over land (2.66K). Additionally, the net turbulent fluxes at the surface and the cloud feedback, while having notable individual contributions to the land and ocean, still did not account for the warmer temperatures over the land when added to the radiative processes. Rather it was the addition of the ocean heat storage/dynamics feedback contribution to the formerly mentioned contributions that resulted in a global-mean land warming of 2.15K and ocean warming of 1.28K. The remaining terms, atmospheric dynamics and offline error, contribute very little with a combined warming of 0.14K and 0.12K to the land and ocean, respectively, bringing the total global warming to 2.29K over land and 1.4K over the ocean.

CHAPTER FIVE

SUMMARY AND CONCLUSIONS

This study applies the CFRAM technique to the land/sea surface temperature contrast given by a transient 1% yr^{-1} CO_2 increase climate simulation of the NCAR CCSM4, to facilitate the quantifiable analysis of the individual contributions from radiative and non-radiative feedback processes. This provides a unique advantage because it helps to identify the significance of the external forcing and the feedbacks with respect to the land and the ocean separately. The results indicate thatCO_2, water vapor and the atmospheric dynamics feedbacks have similar effects for both the land and ocean and that the water vapor feedback and external forcing are the largest contributors to the global-mean surface warming, with the land warming 1.13K and 1.18K and the ocean warming 1.23K and 1.05 K, respectively. The cloud feedback also provides a weak positive contribution to global warming over the land, 0.7K, mainly due to a reduction in clouds and a resultant increase in the absorbed surface shortwave radiation. Also, the cloud feedback closely mimics the shortwave component meridionally, with a cooling (warming) contribution for the ocean (land); however the effect of the longwave component is also evident through the polar warming.

Moreover, this study also support the findings from previous studies, which found that the warming ratio was primarily due to the enhanced evaporative cooling over the ocean, given that the latent heat flux feedback contributed -1.15K towards global-mean temperature change for the ocean surface. However, the most significant temperature change variation between the land and the ocean was actually found to be due to sensible heat flux feedback (2.02K), which inferred that the increased evaporation over the ocean was not the single contributor to the observed warming ratio being greater than unity. Through the analysis of the individual

feedbacks, we were able to discern that the ocean dynamics/heat storage feedback accounted for a large portion of the greater land warming since it cooled the oceans globally by -0.87K and also helped to counteract the ocean warming from the ice-albedo feedback in the upper mid-latitudes. This oceanic cooling is mainly due to the heat storage and the energy uptake facilitated by the ocean dynamics.

Overall, the external forcing, latent heat flux, cloud and ocean dynamics/heat storage feedbacks are the main supporters of the known land/sea warming contrast. The inferences made from this study can be used to provide a better understanding of the climate feedbacks that are important for the land and the ocean in a warming climate, respectively as well as collectively. However, there are two caveats that must be stated, the results from this study are representative of only the NCAR CCSM4 model and thus to gain more generalized and robust results a study using a multi-model ensemble should be done. Also, the aforementioned studies, Dong et al. (2009), Joshi et al. (2008), Sutton et al. (2007) and Manabe et al. (1991), noted that the land/sea warming contrast exists in both the equilibrium and transient states, but the results of this study are solely based on the transient climate response. Thus a reanalysis of the contribution by the ocean heat storage feedback when the heat stored by the oceans in the transient state is released at equilibrium would immensely improve our understanding of the land sea warming ratio and its invariability between the transient and equilibrium states.

REFERENCES

Boer, G. J. (2011), The ratio of land to ocean temperature change under global warming, Climate Dyn., 37, 2253-2270.

Bony S., R. Colman, V.M. Kattsov, R.P. Allan, C.S. Bretherton, J-L. Dufresne, A. Hall, S. Hallegatte, M.M. Holland, W. Ingram, D.A. Randall, B.J. Soden, G. Tselioudis, and M.J. Webb, 2006: How Well Do We Understand and Evaluate Climate Change Feedback Processes? J. Climate, 19, 3445-3482.

Cai, M., and J. Lu, 2009: A new framework for isolating individual feedback processes in coupled general circulation climate models. Part II: Method demonstrations and comparisons. Clim. Dyn., doi: 10.1007/s00382-008-0424-4.

Cess, R.D., and Coauthors, 1990: Intercomparison and interpretation of cloud-climate feedback processes in nineteen atmospheric general circulation models. J. Geophys. Res., 95, 16601-16615.

Cess, R.D., and Coauthors, 1996: Cloud feedback in atmospheric general circulation models: An update. J. Geophys. Res., 101, 12791-12794.

Dong, B., J. M. Gregory, R. T. Sutton (2009), Understanding land-sea warming contrast in response to increasing greenhouse gases. Part I: transient adjustment. J. Climate, 22, 3079-3097.

Fu, Q., and K.N. Liou, 1992: On the correlated k-distribution method for radiative transfer in nonhomogeneous atmosphere. J. Atmos. Sci., 49, 2139-2156.

Fu, Q., and K.N. Liou, 1993: Parameterization of the radiative properties of cirrus clouds. J. Atmos. Sci., 50, 2008-2025.

Hall, A., and S. Manabe, 1999: The Role of Water Vapor Feedback in Unperturbed Climate Variability and Global Warming. J. Climate, 12, 2327-2346.

Hall, A., 2004: The Role of Surface Albedo Feedback in Climate. J. Clim., 17, 1550-1568.

Joshi, M. M., J. M. Gregory, M. J. Webb, D. M. H. Sexton, and T. C. Johns (2008a), Mechanisms for the land/sea warming contrast exhibited by simulations of climate change, Climate Dyn., 30, 455-465.

Joshi, M. M., J. M. Gregory (2008b), Dependence of the land-sea contrast in surface climate response on the nature of the forcing, Geophys. Res. Lett., 35, L24802, doi: 10.1029/2008GL036234.

Lambert, F. H., and J. C. H. Chiang (2007): Control of land-ocean temperature contrast by ocean heat uptake. Geophys. Res. Lett., 34, L13704, doi:10.1029/2007GL029755.

Lu, J., and M. Cai, 2009: A new framework for isolating individual feedback processes in coupled general circulation climate models. Part I: formulation. Clim. Dyn., doi: 10.1007/s00382-008-0425-3.

Manabe, S., and Stouffer R.J., 1980: Sensitivity of a Global Climate Model to an Increase of CO2 Concentration in the Atmosphere. J. Geophys. Res., 85 (C10), 5529-5554.

Manabe, S., R. J. Stouffer, M. J. Spellman, K. Bryan (1991), Transient responses of a coupled ocean-atmosphere model to gradual changes of atmospheric CO2 part 1: annual mean response. J. Climate, 4, 785-818.

Meehl, G.A., T.F. Stocker, W.D. Collins, P. Friedlingstein, A.T. Gaye, J.M. Gregory, A. Kitoh, R. Knutti, J.M. Murphy, A. Noda, S.C.B. Raper, I.G. Watterson, A.J. Weaver and Z.-C. Zhao, 2007: Global Climate Projections. In: Climate Change 2007: The Physical Science Basis. Contribution of Working Group I to the Fourth Assessment Report of the Intergovernmental Panel on Climate Change [Solomon, S., D. Qin, M. Manning, Z. Chen, M. Marquis, K.B. Averyt, M. Tignor and H.L. Miller (eds.)]. Cambridge University Press, Cambridge, United Kingdom and New York, NY, USA.

Ramanathan, V., M.S. Lian, and R.D. Cess, 1979: Increased Atmospheric CO2: Zonal and Seasonal Estimates of the Effect on the Radiation Energy Balance and Surface Temperature. J. Geophys. Res., 84, 4949-4958.

Sejas, S. A., Attributing Contributions to the Seasonal Cycle of Anthropogenic Warming in a Simple Radiative-Convective Global Energy Balance Model (2011). Electronic Theses, Treatises and Dissertations. Paper 278.

Sejas, S. A., M. Cai, A. Hu, G. A. Meehl, W. Washington, P. C. Taylor (2014), Individual feedback contributions to the seasonality of surface warming, Submitted to J. Climate.

Sejas, S. A., O. Albert, M. Cai, T. Deng (2014), Feedback attribution of the land/sea warming contrast, Submitted to J. Geophys. Res.

Soden, B. J., and I. M. Held (2006), An assessment of climate feedbacks in coupled ocean-atmosphere models, J. Climate, 19, 3354-3360.

Soden, B.J., I.M. Held, R. Colman, K.M. Shell, J.T. Kiehl, and C.A. Shields, 2008: Quantifying Climate Feedbacks Using Radiative Kernels. J. Climate, 21, 3504-3520.

Sutton, R. T., B. Dong, J. M. Gregory (2007), Land-sea warming ratio in response to climate change: IPCC AR4 model results and comparison with observations, Geophys. Res. Lett., 115, L02701, doi:10.1029/2006GL028164.

Taylor, P.C., M. Cai, A. Hu, J. Meehl, W. Washington, and G. J. Zhang (2013), A decomposition of feedback contributions to polar warming amplification, J. Climate, 26, 7023-7043.

Trenberth, K.E., P.D. Jones, P. Ambenje, R. Bojariu, D. Easterling, A. Klein Tank, D. Parker, F. Rahimzadeh, J.A. Renwick, M. Rusticucci, B. Soden and P. Zhai, 2007: Observations: Surface and Atmospheric Climate Change. In: Climate Change 2007: The Physical Science Basis. Contribution of Working Group I to the Fourth Assessment Report of the Intergovernmental Panel on Climate Change [Solomon, S., D. Qin, M. Manning, Z. Chen, M. Marquis, K.B. Averyt, M. Tignor and H.L. Miller (eds.)]. Cambridge University Press, Cambridge, United Kingdom and New York, NY, USA.

Wetherald, R.T., and S. Manabe, 1988: Cloud feedback processes in a general circulation model. J. Atmos. Sci., 45, 1397-1415.

BIOGRAPHICAL SKETCH

Oriene Saphique Albert was born on December 31, 1985 in St. John's, Antigua to her dear parents Bernard and Patricia. At age 20 she moved to the USA alone to study meteorology at the University of South Alabama in Mobile, AL from 2006-2009. In 2009 she graduated Cum Laude with a Bachelor of Science in Meteorology, while holding three part-time jobs.

Oriene's interest in meteorology ignited at the age of 10, when Hurricane Luis struck Antigua. After completing her undergraduate degree she worked as a Research Technologist for the Center for Hurricane Intensification and Landfall Investigation at the University of South Alabama before moving to Florida State University to pursue a Master of Science degree. During her time at Florida State University she was a teaching assistant and also did climate research under the guidance of Dr. Ming Cai.